Eur. Phys. J. B **40**, 327–335 (2004)
DOI: 10.1140/epjb/e2004-00270-2

THE EUROPEAN PHYSICAL JOURNAL B

Influence of evaporation on Bénard-Marangoni instability in a liquid-gas bilayer with a deformable interface

C. Moussy, G. Lebon, and J. Margerit[a]

University of Liège, Institute of Astrophysics, Geophysics, and Oceanography, B-5, Sart-Tilman, 4000 Liège, Belgium

Received 10 May 2003 / Received in final form 9 February 2004
Published online 31 August 2004

Abstract. Bénard-Marangoni instability in a bilayer liquid-gas system with a deformable interface is investigated. The present work is devoted to a linear approach. We discuss the influence on the onset of stability of the following parameters: initial temperature profile, relative thickness of the gas and liquid layers, deformation of the interface, influence of the evaporation process, and the wetting parameter.

PACS. 47.20.Dr Surface-tension-driven instability – 47.20.Hw Morphological instability; phase changes – 05.70.Np Interface and surface thermodynamics – 44.25.+f Natural convection

1 Introduction

It is well known that two different mechanisms are responsible for the appearance of motion in a fluid layer subject to a temperature gradient. These mechanisms are gravity (Rayleigh-Bénard [1] convection) and thermocapillarity (Bénard-Marangoni [2] convection). Thermoconvection induced by these mechanisms was studied by many authors, as for instance, Bénard [3], Chandrasekhar [4] (Rayleigh-Bénard instability) and Pearson [5] (Bénard-Marangoni instability).

For a thin liquid layer in a micro-gravity environment, surface tension is the main driving mechanism of the flow instability. The first analysis of surface deformation effects on thermocapillarity convection was proposed by Scriven and Sterling [6]. The problem of thermocapillary instability coupled with capillary and gravity waves was studied recently by Regnier et al. [7,8], in the linear and nonlinear cases with surface deformation. The deformability provides an additional "degree of freedom" and may have a decisive role mainly in thin layers. The crispation number C_r which is a measure of the deformation must therefore be included as an additional parameter. It was found by Davis and Homsy [9] that the surface deflection stabilizes the system if the buoyancy is dominant and destabilizes the system if surface tension effects are dominant. It was also shown [10] that the system becomes unconditionally unstable with respect to disturbances with wavelengths tending to infinity. It is noteworthy that the above referred works are only concerned with non-evaporating liquid layers.

When evaporation takes place, heat is drawn from the bulk of the layer and reinforces instability. Acting as a cascade effect, the increase of instability leads to an enhancement of the evaporating rate. Bénard-Marangoni instability in an evaporating liquid layer was studied, under a reduced pressure condition, experimentally by Gillon et al. [11], and theoretically for both liquid and vapor phase of infinite depth by Palmer [12]. A linear stability analysis for a rapidly evaporating liquid surface has been carried out by Prosperetti and Plesset [13], and by Burelbach et al. [14] in the non linear case for a one liquid phase with deformable upper surface. Similarity solutions for the period preceding the onset of instability were obtained by Ha [15], his stability analysis was restricted to the linear case to a one layer system with an undeformable upper surface.

The purpose of the present work is to study the onset of Bénard-Marangoni instability in a liquid-gas bilayer under evaporation with a deformable interface. The analysis is restricted to a 2D-approach and the perturbations are assumed to remain infinitesimally small (linear regime). Gravity effects are assumed to be negligible and will not be taken into account.

The paper is organized as follows. In Section 2, the basic balance laws and the boundary conditions are established. The reference solution is derived in the quasi steady approximation in Section 3. The linear stability analysis developed in Section 4 allows to determine the threshold of instability of the evaporating liquid-gas system as a function of various parameters. In Section 5, the numerical results are presented and discussed, and conclusions are drawn in Section 6.

[a] e-mail: Jonathan.Margerit@ulg.ac.be

2 Mathematical formulation

The system is formed by an evaporating liquid layer of infinite longitudinal extent in the x-direction, of initial depth d and lying on a heated rigid horizontal plate (Fig. 1). The liquid is incompressible, Newtonian, and heated from below, the lower plate is maintained at the uniform temperature T_H. The liquid is surmounted by an inert gas (say air) of initial thickness L at pressure p_g. The gas is bounded by a perfectly heat conducting upper plate maintained at temperature T_C. A pump maintains a constant reduced pressure in the gas layer and evacuates the gas (vapor+air). The total distance between the two plates remains constant and is equal to $L + d$.

Subscripts l and g describe the liquid and the gas phases respectively. As the liquid evaporates, the upper gas layer is formed by the mixture of air and liquid vapor, respectively indexed by subscripts air and v. The analysis is carried out in the frame of the Boussinesq approximation. The interface is deformable and subject to a surface tension σ_s that decreases linearly with the temperature T, i.e.,

$$\sigma_s = \sigma_0 - \gamma(T - T_0)$$

where σ_0 is the surface tension at an arbitrary reference temperature T_0, say the temperature T_0 of the ambient atmosphere, $\gamma = -\frac{\partial \sigma_s}{\partial T}\big|_{T_0}$ is equal to minus the rate of change of surface tension with temperature, and is assumed to be positive.

A cartesian coordinate system is selected with its origin located at the bottom of the liquid layer, the z-axis pointing towards the cold plate. The moving liquid-gas interface is described by equation $z = h(t, x)$.

The normal vector $\mathbf{n}$ to the interface, directed towards the gas phase, and the tangential vector $\mathbf{t}$ have the following x, z coordinates:

$$\mathbf{t} = \begin{pmatrix} \frac{1}{\sqrt{1+\eta^2}} \\ 0 \\ \frac{\eta}{\sqrt{1+\eta^2}} \end{pmatrix}, \qquad \mathbf{n} = \begin{pmatrix} \frac{-\eta}{\sqrt{1+\eta^2}} \\ 0 \\ \frac{1}{\sqrt{1+\eta^2}} \end{pmatrix},$$

where $\eta = \frac{\partial h(t,x)}{\partial x}$ denotes the deflection of the interface.

The interfacial normal velocity is given by

$$\mathbf{V}_I.\mathbf{n} = \frac{\partial h(t,x)}{\partial t} / \sqrt{1+\eta^2}. \tag{1}$$

The field equations and the boundary conditions will be put under non-dimensional form by using the following scalings: d for length, d^2/α_l for time, α_l/d for velocity, $\rho_l {\alpha_l}^2/d^2$ for pressure, $\rho_l \alpha_l/d$ for the mass flux where ρ_l and α_l designates the mass density and thermal diffusivity of the liquid respectively. Dimensionless temperature fields are defined through $T^* = \frac{T - T_H}{\frac{h_{lg}}{c_{p_l}}}$. The quantity h_{lg} is the latent heat of evaporation, c_{p_l} is the heat capacity of the liquid at constant pressure.

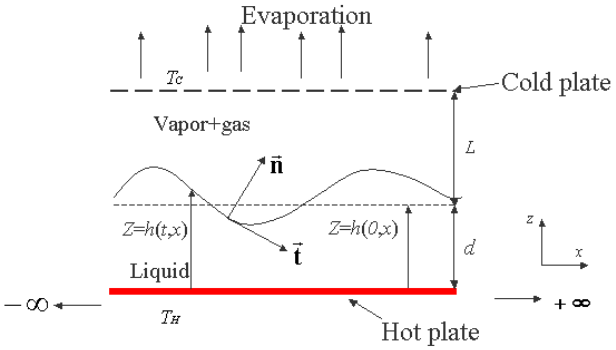

Fig. 1. Physical domain.

In absence of gravity, the dimensionless (indexed by *) governing equations are:

- Liquid phase equations:

$$\boldsymbol{\nabla} \cdot {\mathbf{V}_l}^* = 0, \tag{2}$$

$$P_{r_l}^{-1}[\frac{\partial {\mathbf{V}_l}^*}{\partial t^*} + ({\mathbf{V}_l}^* \cdot \boldsymbol{\nabla}){\mathbf{V}_l}^* + \boldsymbol{\nabla} p_l^*] = \nabla^2 {\mathbf{V}_l}^*, \tag{3}$$

$$\frac{\partial T_l^*}{\partial t^*} + ({\mathbf{V}_l}^* \cdot \boldsymbol{\nabla}) T_l^* = \nabla^2 T_l^*, \tag{4}$$

- Gas phase equations:

$$\boldsymbol{\nabla} \cdot {\mathbf{V}_g}^* = 0, \tag{5}$$

$$P_{r_g}^{-1}\phi_\alpha[\frac{\partial {\mathbf{V}_g}^*}{\partial t^*} + ({\mathbf{V}_g}^* \cdot \boldsymbol{\nabla}){\mathbf{V}_g}^* + \phi_\rho \boldsymbol{\nabla} p_g^*] = \nabla^2 {\mathbf{V}_g}^*, \tag{6}$$

$$\phi_\alpha[\frac{\partial T_g^*}{\partial t^*} + ({\mathbf{V}_g}^* \cdot \boldsymbol{\nabla}) T_g^*] = \nabla^2 T_g^*, \tag{7}$$

$$\phi_\alpha Le[\frac{\partial Y_v^*}{\partial t^*} + ({\mathbf{V}_g}^* \cdot \boldsymbol{\nabla}) Y_v^*] = \nabla^2 Y_v^*, \tag{8}$$

where the symbols $\mathbf{V}^* = (u^*, v^*, w^*)$, p^*, T^* represent the nondimensional velocity, pressure and temperature fields respectively, Y_v^* is the mass fraction of liquid vapor (already nondimensional), and is linked with the mass fraction of the air by the relation $Y_{air}^* + Y_v^* = 1$. The quantity $P_{r_l} = \frac{\mu_l}{\rho_l \alpha_l}$ is the Prandtl number of the liquid, where μ_l is the dynamic viscosity, $P_{r_g} = \frac{\mu_g}{\rho_g \alpha_g}$ is the Prandtl number of the gas, $\phi_\alpha = \frac{\alpha_l}{\alpha_g}$ is the ratio of the thermal diffusivities of the liquid and the gas, $\phi_\rho = \frac{\rho_l}{\rho_g}$ is similarly defined as the ratio of the densities, and finally $Le = \frac{\alpha_g}{\alpha_v}$ is the Lewis number, where α_v designates the diffusion coefficient of the water vapor into the gas.

The relevant dimensionless initial and boundary conditions are:

Initial conditions

At $t = 0$, the depth of the liquid layer is equal to d, the initial temperature and velocity are supposed to be known and independent of the x-coordinate. More precisely, one has $T_l^* = 0$, $T_g^* = constant$, ${\mathbf{V}_g}^* = constant$, ${\mathbf{V}_l}^* = 0$, $Y_v^* = constant$.

Boundary conditions
At the solid impermeable hot wall ($z^* = 0$):

$$T_l^* = 0, \quad \mathbf{V}_l{}^* = 0. \tag{9}$$

At the solid permeable upper plate ($z^* = 1 + l$):

$$T_g^* = T_C^*, \quad Y_v^* = Y_L^*, \quad \mathbf{t}.\boldsymbol{\tau}_g^*\mathbf{n} = 0, \tag{10}$$

where $l = L/d$ is the ratio of initial gas layer depth to the initial liquid layer depth, Y_L^* is a measure of the wetting of the upper plate, and $\boldsymbol{\tau}_g^* = \mu_g((\boldsymbol{\nabla}\mathbf{V}_g{}^*)^T + \boldsymbol{\nabla}\mathbf{V}_g{}^*)$ the viscous tensor with subscript T denoting transposition.

A no stress condition is used for the upper plate because the plate that we consider is permeable and has a high porosity. Note that for a plate with small porosity, a rigidity condition (no-slip) is more appropriate. We have investigated this condition too and have observed that the results are weakly affected by the choice of this condition.

At the interface $z^* = h^*(t^*, x^*)$:

- The continuity of the tangential velocities yields

$$\mathbf{V}_g{}^*.\mathbf{t} = \mathbf{V}_l{}^*.\mathbf{t}. \tag{11}$$

- Continuity of mass flux leads to

$$J^* = \mathbf{V}_l{}^*.\mathbf{n} - \mathbf{V}_I{}^*.\mathbf{n} = (\mathbf{V}_g{}^*.\mathbf{n} - \mathbf{V}_I{}^*.\mathbf{n})\frac{1}{\phi_\rho}, \tag{12}$$

where J^* is the dimensionless interfacial mass flux.

- Impermeability condition:

$$\frac{1}{\phi_\alpha Le\phi_\rho}\nabla Y_v^*.\mathbf{n} = -(1 - Y_v^*)J^*. \tag{13}$$

- Temperature continuity:

$$T_i^* = T_l^* = T_g^*, \tag{14}$$

where T_i^* is the non dimensional temperature at the interface.

- Balance of energy:

$$J^* = \frac{1}{\phi_\lambda}\nabla T_g^*.\mathbf{n} - \nabla T_l^*.\mathbf{n}, \tag{15}$$

where $\phi_\lambda = \dfrac{\lambda_l}{\lambda_g}$ is the thermal conductivity ratio.

- Continuity of shear stress:

$$\mathbf{t}.\boldsymbol{\tau}_g^*\mathbf{n} - \phi_\mu\mathbf{t}.\boldsymbol{\tau}_l^*\mathbf{n} = M_a\phi_\mu\nabla_\parallel T_l^*, \tag{16}$$

where $\phi_\mu = \dfrac{\mu_l}{\mu_g}$ is the viscosity ratio, $\nabla_\parallel$ the interfacial gradient, and

$$M_a = -\frac{\partial\sigma_s}{\partial T}\frac{h_{lg}d}{c_{p_l}\alpha_l\mu_l}$$

the dimensionless Marangoni number as defined by Ha [13]. M_a has a fixed value for a given fluid provided the initial liquid depth is fixed. For further purpose, we introduce also the crispation number $C_r = \dfrac{\mu_l\alpha_l}{d\sigma_0}$, which measures the deformability of the interface. For a given fluid, the parameters M_a and $\dfrac{1}{C_r}$ are both proportional to the initial depth d and do not depend of any other parameters, like temperature T_H ot T_C, so that this Marangoni number M_a, as defined by Ha, and the crispation number C_r are not independent.

- Normal stress balance:

$$p_g^* - p_l^* = P_{r_l}\left(\frac{1}{\phi_\mu}\mathbf{t}.\boldsymbol{\tau}_g^*\mathbf{n} - \mathbf{t}.\boldsymbol{\tau}_l^*\mathbf{n}\right) + J^*(\mathbf{V}_g{}^*.\mathbf{n} - \mathbf{V}_l{}^*.\mathbf{n}) - \mathcal{C}^*\frac{P_{r_l}}{C_r}\frac{\sigma_s}{\sigma_o}, \tag{17}$$

where $\mathcal{C}^* = \nabla.\mathbf{n}$ is the curvature of the interface, and

$$\frac{\sigma_s}{\sigma_o} = 1 - M_aC_r(T_i^* - T_0^*),$$

Assuming that the vapor is satured at the interface, one obtains from the equality of the chemical potentials at the interface, the following relation for the interfacial vapor mass fraction Y_i^* [13]:

$$Y_i^* = \frac{\exp\left[\dfrac{c_{p_l}}{\Re}\left(\dfrac{1}{T_b^* + \dfrac{c_{p_l}T_H}{h_{lg}}} - \dfrac{1}{T_i^* + \dfrac{c_{p_l}T_H}{h_{lg}}}\right)\right]}{r_w - (r_w - 1)\exp\left[\dfrac{c_{p_l}}{\Re}\left(\dfrac{1}{T_b^* + \dfrac{c_{p_l}T_H}{h_{lg}}} - \dfrac{1}{T_i^* + \dfrac{c_{p_l}T_H}{h_{lg}}}\right)\right]}, \tag{18}$$

the undefined quantities $\Re$, $r_w = \dfrac{M_{air}}{M_l}$ and T_b^* are respectively the universal gas constant, the ratio of the molecular weights of air and liquid, and the nondimensional boiling temperature of the liquid.

3 Quasi-steady solution in the reference state

Here we work within the quasi-steady approximation which means that the time derivatives in the partial differential equations for both the liquid and gas phases are zero except in the interfacial kinematical condition (1). The set of equations (1–18) is characterized by a so-called reference one dimensional solution independent of the x^* coordinate. Continuity equations (2) and (5) lead to a null velocity in the liquid phase and to a constant velocity in the gas phase. The pressures are uniform. The temperature profile is linear with respect to z^* in the liquid phase,

but non linear in the gas phase, namely:

$$T_l^*(z^*,t^*) = T_i^* + \frac{T_i^*}{h^*(t^*)}(z^* - h^*(t^*)), \tag{19}$$

$$T_g^*(z^*,t^*) = T_i^* - (T_i^* - T_C^*) \times \frac{1 - \exp\left[\phi_\alpha \left(w_g^* - \frac{\partial h^*(t^*)}{\partial t^*}\right)(z^* - h^*(t^*))\right]}{1 - \exp\left[\phi_\alpha \left(w_g^* - \frac{\partial h^*(t^*)}{\partial t^*}\right) L^*(t^*)\right]}, \tag{20}$$

where $L^*(t^*) = 1 + l - h^*(t^*)$. According to relations (10) and (13) the expression of the mass fraction is given by

$$Y_v^*(z^*,t^*) = 1 + (Y_L^* - 1) \times \exp\left[\phi_\alpha Le \left(w_g^* - \frac{\partial h^*(t^*)}{\partial t^*}\right)(z^* - l - 1)\right]. \tag{21}$$

Combining this relation with (12), one obtains at the interface the following relation between J^* and Y_i^*:

$$J^* = \frac{1}{\phi_\alpha Le \phi_\rho L^*(t^*)} \log\left(\frac{1 - Y_L^*}{1 - Y_i^*}\right), \qquad \forall t^*. \tag{22}$$

From the energy balance equation (15), the temperature profiles (19) and (20), and the definition (12), it is found that

$$J^* = \frac{1}{\phi_\lambda}(T_i^* - T_C^*)\frac{\phi_\alpha J^* \phi_\rho}{1 - \exp(\phi_\alpha J^* \phi_\rho L^*(t^*))} - T_i^* \frac{1}{h^*(t^*)}, \qquad \forall t^*. \tag{23}$$

The resolution of the set of three equations (18), (22), and (23), involving the three unknowns quantities T_i^*, Y_i^* and J^* allows us to determine the mass flux J^*, as a function of the liquid height parameter $h^*(t)$ at any instant of time. Since in virtue of expression (12), one has

$$J^* = -\frac{\partial h^*(t^*)}{\partial t^*}, \tag{24}$$

one obtains after integration an expression for the evolution $h^*(t)$ of the evaporating liquid layer depth as a function of time. For a given fluid, the reference state depends on the four non dimensional parameters $T_H \frac{c_{pl}}{h_{lg}}$, T_C^*, l, and Y_L.

4 Stability analysis

In this section, we study the stability of the reference solution derived in the previous section in view to determine the onset of instability. As only infinitesimally small disturbances are considered, the analysis is strictly linear. Superscript " ' " denotes the perturbed quantities, namely $G' = G^* - G_r^*$. In addition, it is assumed that the basic solution, indexed r, remains frozen during the stability analysis.

By applying the divergence operator on the Navier-Stokes equations, and using the continuity equation, we can eliminate the horizontal component velocity, we are then left with the following set of unknowns (w', p', T'), both in the liquid and gas phase, complemented by Y_v' and h'.

According to the classical procedure, these quantities are expanded in normal modes, i.e. explicitly

$$\begin{pmatrix} w_l'(x,z,t) \\ w_g'(x,z,t) \\ T_g'(x,z,t) \\ T_l'(x,z,t) \\ p_l'(x,z,t) \\ p_g'(x,z,t) \\ Y_v'(x,z,t) \\ h'(x,t) \end{pmatrix} = \exp(\sigma t + ikx) \begin{pmatrix} \tilde{w_l}(z) \\ \tilde{w_g}(z) \\ \tilde{T_g}(z) \\ \tilde{T_l}(z) \\ \tilde{p_l}(z) \\ \tilde{p_g}(z) \\ \tilde{Y_v}(z) \\ \tilde{\Lambda} \end{pmatrix},$$

the quantity k is the wave number, σ is the growth rate of the disturbance which determines the degree of amplification or damping, the z-dependent quantities are the so-called amplitudes. For simplicity, we omit the superscripts tilda and star *, and use the following approximation $\phi_\rho - 1 \approx \phi_\rho$.

Under these restrictions, we obtain the following linearized relations for the amplitudes:

– liquid-gas phase equations:

$$(D^2 - k^2)p_l = 0, \tag{25}$$

$$(D^2 - k^2)p_g = 0, \tag{26}$$

$$P_{r_l}^{-1}[\sigma w_l + D p_l] = (D^2 - k^2)w_l, \tag{27}$$

$$P_{r_g}^{-1}\phi_\alpha[(\sigma + \phi_\rho J_r D)w_g + \phi_\rho D p_g] = (D^2 - k^2)w_g, \tag{28}$$

$$\phi_\alpha[(\sigma + \phi_\rho J_r D)T_g + w_g D T_{g,r}] = (D^2 - k^2)T_g, \tag{29}$$

$$\sigma T_l + w_l D T_{l,r} = (D^2 - k^2)T_l, \tag{30}$$

$$\phi_\alpha Le\,[(\sigma + \phi_\rho J_r D)Y_v + w_g D Y_{v,r}] = (D^2 - k^2)Y_v, \tag{31}$$

where D stands for d/dz.

– Wall boundary conditions:

$$z = 0: \qquad T_l = w_l = D w_l = 0, \tag{32}$$

$$z = 1 + l: \qquad T_g = w_g = Y_v = (D^2 + k^2)w_g = 0. \tag{33}$$

– Interfacial conditions ($z = h_r(t_r)$):

$$D w_l - D w_g = w_{g,r} k^2 \Lambda, \tag{34}$$

$$J\phi_\rho = \phi_\rho(w_l - \sigma\Lambda) = w_g - \sigma\Lambda, \tag{35}$$

$$\frac{1}{Le\phi_\alpha} D Y_v = (Y_{i,r} - 1)(w_g - \sigma\Lambda) + Y_v(h_r(t_r))J_r\phi_\rho, \tag{36}$$

$$T_l - T_g = (D T_{g,r} - D T_{l,r})\Lambda, \tag{37}$$

$$\frac{1}{\phi_\rho}(w_g - \sigma\Lambda) = \frac{1}{\phi_\lambda} DT_g - DT_l + \Lambda\left(\frac{1}{\phi_\lambda} D^2 T_{g,r} - D^2 T_{l,r}\right), \quad (38)$$

$$(k^2 + D^2)(-w_g + \phi_\mu w_l) = -Mak^2\phi_\mu (T_l + DT_{l,r}\Lambda), \quad (39)$$

$$p_g - p_l = 2P_{r_l}\left(\frac{1}{\phi_\mu} Dw_g - Dw_l\right) - 2J_r(w_g - w_l) - \frac{k^2 P_{r_l}}{C_r}\Lambda\frac{\sigma_s}{\sigma_o}, \quad (40)$$

$$Y_v = \left(\frac{df(T_{l,r})}{dT_{l,r}} DT_{l,r} - DY_{v,r}\right)\Lambda + \frac{df(T_{l,r})}{dT_{l,r}} T_l, \quad (41)$$

where

$$f(T_{l,r}) = \frac{\exp\left[\frac{c_{pl}}{\Re}\left(\frac{1}{T_b^* + \frac{c_{pl}T_H}{h_{lg}}} - \frac{1}{T_{l,r} + \frac{c_{pl}T_H}{h_{lg}}}\right)\right]}{r_w - (r_w - 1)\exp\left[\frac{c_{pl}}{\Re}\left(\frac{1}{T_b^* + \frac{c_{pl}T_H}{h_{lg}}} - \frac{1}{T_{l,r} + \frac{c_{pl}T_H}{h_{lg}}}\right)\right]}. \quad (42)$$

Observe that the particular case of an undeformable surface is directly treated by setting $\Lambda = 0$ and by disregarding the normal force balance equation (40). A remark is in form concerning the boundary condition (37) which seems to be in contradiction with the boundary condition (14) $T_l^* = T_g^*$. The latter is truly satisfied at the liquid-gas deformed interface of equation $z^* = h^*(t^*, x^*)$. This is not in conflict with equation (37) as the latter refers to the boundary condition to be satisfied by the linearized perturbation on the *flat reference interface* of equation $z = h_r(t_r)$. Expression (37) represents the price to be paid for the linearization modeling. The jump in (37) is the consequence of the presence of a deformed interface, whose exact position is described by $h_r(t_r) + \Lambda\exp(\sigma t + ikx)$. In absence of deformation ($\Lambda = 0$), one recovers the result $T_l^* = T_g^*$ as it should. All the relations (34) to (41) have a right term proportional to Λ which is of the same kind that the term appearing in relation (37) when dealing with the interface deformation.

The linear differential set of equations (25–42) has non trivial solutions that can be found numerically. We are faced with an eigenvalue problem from which we are able to determine the marginal stability curves M_a versus k corresponding to $\sigma = 0$, for the four other independent parameters $T_H\frac{c_{pl}}{h_{lg}}$, T_C^*, l, and Y_L fixed; in the present work, exchange of stability is taken for granted.

5 Results and comments

In our calculations, we have considered two different fluids: water and ethanol. The essential difference is that ethanol is more volatile than water. The ambient reference dimensional temperature T_0 is equal to 30 °C. The surface tension σ_0 for this dimensional temperature is of the order of 10^{-2} N/m for both liquids. The inert gas is, as stated before, assumed to be air.

We will discuss the role of some parameters on the onset of motion. In particular, we examine the effect of the value of the temperature T_H imposed at the bottom heating plate, the ratio of the initial gas layer depth to the initial liquid layer depth l, and the mass fraction of liquid vapor Y_L evacuated through the upper boundary.

It is well known that in presence of surface deformations, we are faced with two kinds of instabilities: the 'classical' short wavelength Marangoni mode correspond to critical wave-numbers close to two and the long wave mode instability for which the wave-number tends to zero. In the latter situation, the deformation was shown to be destabilizing in the absence of evaporation [5,6]. We will see that these two kinds of instabilities are still present when there is evaporation with a deformable interface. Figure 2 shows marginal stability curves M_a versus k for different values of the hot plate temperature T_H. The marginal stability curves C_r versus k are obviously derived from the $M_a(k)$ curves because C_r and M_a are linked by the relation $C_r = \frac{\alpha_r}{M_a}$ where the coefficient $\alpha_r = \frac{\gamma h_{lg}}{c_{pl}\sigma_0}$ is known for a given fluid. We have verified that the unstable domain is the domain above the neutral stability curve $M_a(k)$ by studying some non null growth rate σ.

First, we notice that an increase of the temperature at the bottom plate has a destabilizing effect. Indeed, for a bottom plate temperature such that $T_C = T_H = 50$ °C, with $Y_L = 0$, $l = 1$, $h_r^* = 1$, the curve of neutral stability is below the one corresponding to $T_H = T_C = 30$ °C, (see Fig. 2).

For different values of the temperature at the bottom and the top plates, it is the temperature at the lower boundary which is the more influent. For example if $T_C = 30$ °C, and $T_H = 60$ °C the neutral stability curve behaves as in the case $T_H = T_C = 60$ °C. We therefore conclude that the temperature of the gas at the upper plate has only a slight effect on the onset of instability. Observe that in the case $T_H = T_C$, the evaporation process absorbs heat, and therefore, there exists a temperature gradient through the liquid layer which is the source of instability. It appears also that the most dangerous mode occurs at small values of k.

When the temperature at the boundaries is maintained at $T_H = T_C = 30$ °C, and the mass fraction of liquid vapor $Y_L = 0$, then by increasing the ratio l we find that the curve of neutral stability moves towards larger critical Marangoni values, as exhibited by Figure 3. It means that the system is more stable when l is increased. As a consequence of the increase of l, the interfacial mass flux J becomes smaller and smaller.

The behaviour of the system at small wave numbers is represented in Figure 4. It is observed that instability

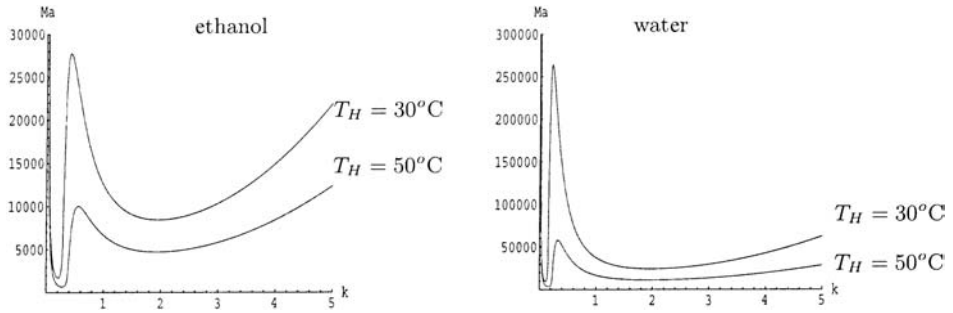

Fig. 2. Neutral stability curves, M_a versus k, for ethanol and water: role of the temperature of the lower plate, $T_C = T_H$, $l = 1, \quad Y_L = 0, \quad h_r^* = 1$.

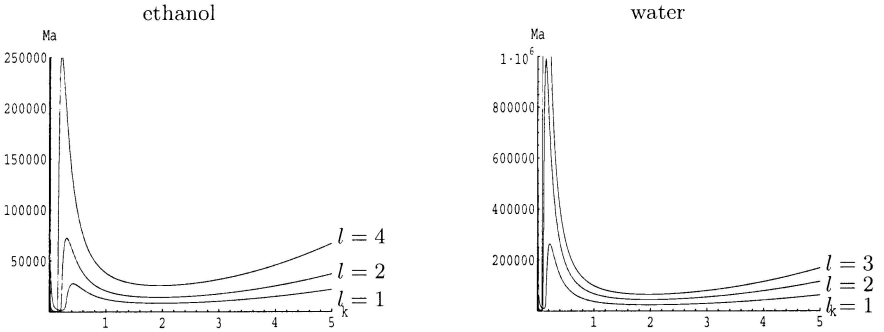

Fig. 3. Neutral stability curves: role of the relative thickness between the gas and liquid, $T_H = T_C = 30$ °C, $Y_L = 0$, $h_r^* = 1$.

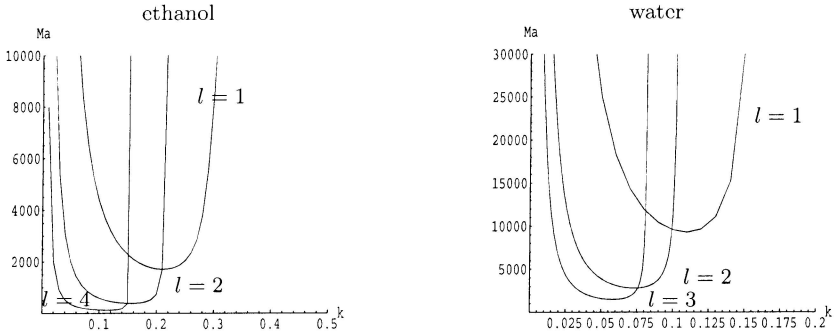

Fig. 4. The same as in Figure 3 but for small values of k.

is increased when l is growing, while conversely, for large wave numbers, it is for large l values that system is more stable.

We have also investigated the role of the mass fraction Y_L at the upper plate on instability. Let $T_H = T_C = 30$ °C and $l = 1$. For this temperature-value, an increase of Y_L has a stabilizing effect in the case of ethanol as well as of water (see Fig. 5). In the case of ethanol (resp. in the case of water) for an initial liquid layer depth of $d = 10^{-4}$ m, the Marangoni number value is $M_a = 66794$ (resp. 147 882). This value is shown in Figure 5 by an horizontal straight line. For this value the crispation number C_r is 4.8×10^{-5}. For $0.14477 > Y_L > 0.126$ the basic solution is always stable for the short wave modes. For $Y_L > 0.14477$ we have condensation and the interfacial mass flux J has a negative value. In Figure 6 which is a magnification of Figure 5, we report the results in the region of small wave numbers: the system is more unstable when Y_L is decreased and is the most unstable for $Y_L = 0$. A similar behaviour is observed with water.

To illustrate the behaviour of the non trivial solutions of the eigenvalue value problem, we have represented in the $x - z$ plane the non dimensional isothermal lines and the velocity field of the perturbed quantities for an ethanol layer surmounted by air (see Fig. 7). We have taken $T_C = T_H = 30$ °C, $l = 1$, $Y_L = 0.126$. The corresponding critical Marangoni and wave numbers are $M_a = 66794$, and $k_c = 1.99$.

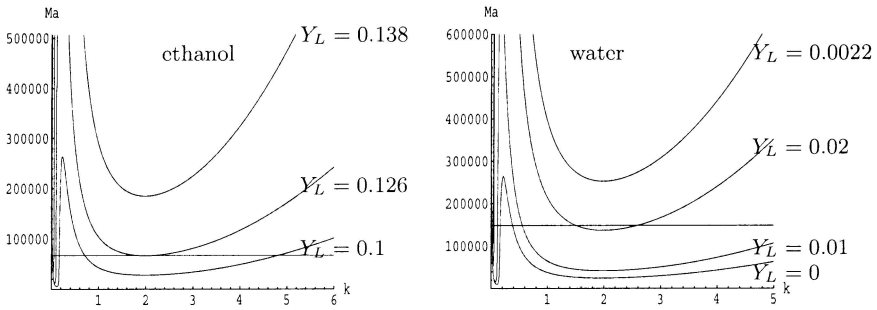

Fig. 5. Neutral stability curves: role of the upper plate mass fraction of liquid vapor influence, $T_C = T_H = 30$ °C, $h_r^* = 1$, $l = 1$.

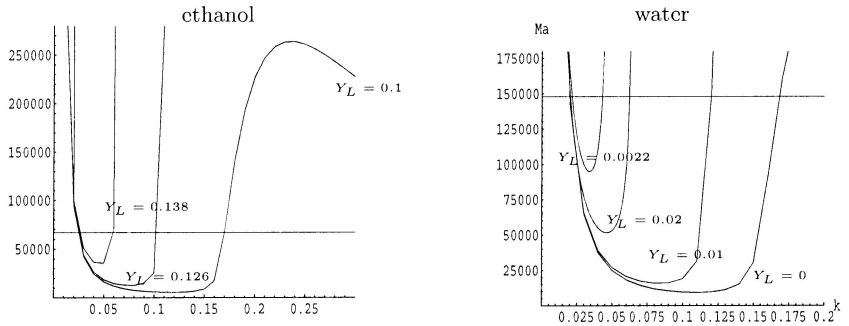

Fig. 6. The same as in Figure 5 but for small values of k.

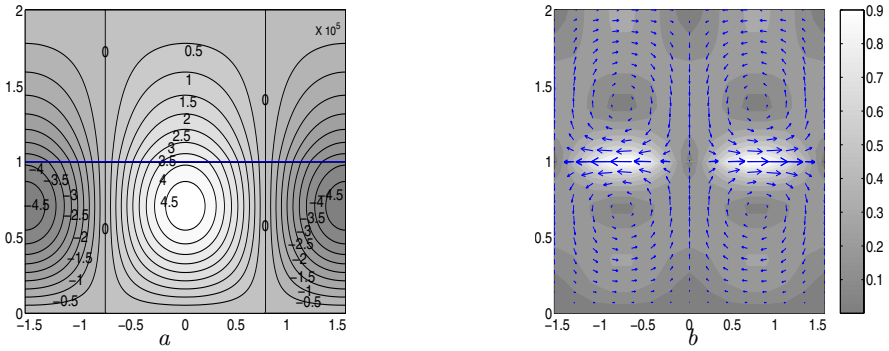

Fig. 7. Long wave number mode: (a) Isothermal lines, (b) Velocity fields, $T_H = T_C = 30$ °C, $l = 1$, $Y_L = 0.126$, $M_a = 66794$, and $k = 1.99$. (Ethanol.)

The initial depth of the liquid layer is $d = 10^{-4}$ m: for this value, the crispation number C_r is 4.8×10^{-5} for ethanol. The corresponding neutral stability curve in this case is represented in Figure 5. In Figure 7b for the velocity fields, bright regions correspond to large velocity fields and darker regions to slower velocities. We have normalized the linear perturbed fields by the maximum intensity of the liquid velocity at the interface. The velocity is larger in the liquid than in the gas. The perturbed temperature values are very small so that we have multiplied their actual values by a factor 10^5 as is indicated in the figure. The convection cells are seen to be well developed and the maximum of the velocity corresponds to the minimum of the temperature. The deformation of the interface is negligible for this wave number.

Figure 8 reproduces the temperature and velocities fields for the same parameters as above ($M_a = 66794$, $Y_L = 0.126$) but now for the small wave number $k = 0.1$ that corresponds to another non trivial solution of the eigenvalue problem. We have divided the actual gas phase velocity values by a factor 5 for convenience. The deformation of the interface is also sketched with the isothermal lines. The deformation is important for this value of k. This leads to a jump of the perturbed temperature through the reference interface, (cf. Eq. (37)). The maximum of the velocity corresponds also to the minimum of the temperature, but contrary to the critical wave number of Figure 5, the velocity now, is higher in the gas phase than in the liquid phase.

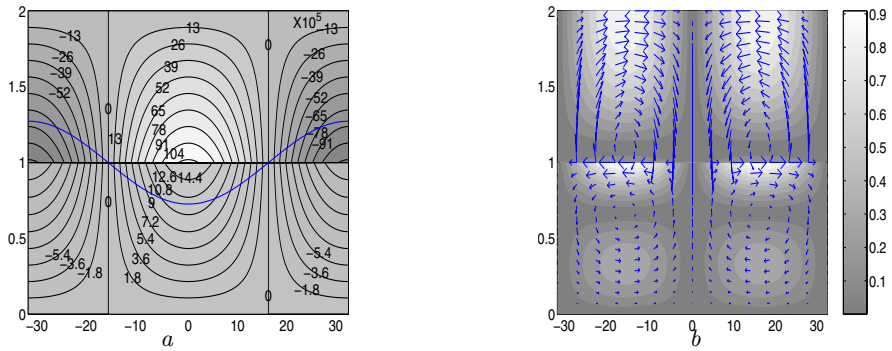

Fig. 8. Short wave number mode: (a) Isothermal lines, (b) Velocity fields, $T_H = T_C = 30$ °C, $l = 1$, $Y_L = 0.126$, $M_a = 66794$, and $k = 0.1$. (Ethanol.)

6 Conclusions

Our objective was to study the onset of thermo-convective instability in an evaporating liquid layer heated from below and surmounted by a non reacting gas. In addition the liquid-gas interface is allowed to be deformable. Under microgravity and the quasi-steady approximation, a linear approach is carried out. We highlight the stabilizing and destabilizing effects, by varying some parameters like the relative depth of the gas and liquid layers, the temperature at the bottom plate, and the mass fraction coefficient. The results are presented and analyzed, for both the short and long wave-lengths. It appears that evaporation and deformation play a determinant role. The effect of evaporation is essentially destabilizing while deformation of the interface gives rise to marginal curves with two minima: one located at small value of k close to zero, the other one located around $k = 2$. In most cases, the mode close to $k = 0$ is the most unstable. Of course many problems remain open like the coupled effect of gravity and surface-tension driven instability, and a study of the transitory regime preceding the occurrence of the steady study. It would also be interesting to compare our results with experimental data. But to our knowledge, no much data are available.

7 Nomenclature

c_{p_l}	Heat capacity of the liquid
c_{p_g}	Heat capacity of the gas
$C_r = \frac{\mu_l \alpha_l}{\sigma_s d}$	Crispation number
d	Depth of the liquid layer
$h_{lg} = h_g - h_l$	Latent heat of evaporation
J	Interfacial mass flux
k	Wave number of disturbances
$Le = \frac{\alpha_g}{\alpha_v}$	Lewis number
$M_a = -\frac{\partial \sigma}{\partial T_l^*} \frac{h_{lg} d}{c_{p_l} \alpha_l \mu_g}$	Marangoni number
M_{air}	Molecular weight of air
M_l	Molecular weight of liquid
$P_{r_l} = \frac{\mu_l}{\rho_l \alpha_l}$	Prandtl number of the liquid
$P_{r_g} = \frac{\mu_g}{\rho_g \alpha_g}$	Prandtl number of the gas
$r_\omega = \frac{M_{air}}{M_l}$	Weight molecular ratio
$\Re$	Universal gas constant
T_b	Boiling temperature of liquid
T_C	Temperature at the cold upper plate
T_H	Temperature at the hot lower plate
T_i	Interfacial temperature
u_l, v_l, w_l	Coordinates of the vector velocity
V_I	Interfacial velocity
$Y_v = \frac{\rho_v}{\rho_g}$	Mass fraction of liquid vapor
$\alpha_l = \frac{\lambda_l}{\rho_l c_{p_l}}$	Thermal diffusivity of the liquid
$\alpha_g = \frac{\lambda_g}{\rho_g c_{p_g}}$	Thermal diffusivity of the gas
α_v	Mass diffusivity
λ_g	Thermal conductivity of gas
λ_l	Thermal conductivity of liquid
μ_l	Dynamic viscosity of the liquid
μ_g	Dynamic viscosity of the gas
ρ_l	Density of the liquid
ρ_g	Density of the gas
σ	growth rate
$\phi_\alpha = \frac{\alpha_l}{\alpha_g}$	Thermal diffusivity ratio
$\phi_\rho = \frac{\rho_l}{\rho_g}$	Density ratio
$\phi_\lambda = \frac{\lambda_l}{\lambda_g}$	Thermal conductivity ratio
$\phi_\mu = \frac{\mu_l}{\mu_g}$	Viscosity ratio

This work was supported by the ICOPAC EC programme HRPN CT 2000-00136 and ESA CIMEX and PRODEX projects. Fruitful discussions with P. Colinet (Free University Brussels) are acknowledged.

References

1. L. Rayleigh, Philos. Mag. **32**, 529 (1916)
2. C. Marangoni, *On the expansion of a drop of liquid floating on the surface of another liquid* (Tipographia dei fratelli Fusi, Pavia, 1865)
3. H. Bénard, Rev. Gen. Sci. Pures Appl. **11**, 1261 (1900); H. Bénard, Rev. Gen. Sci. Pures Appl. **11**, 1309 (1900)
4. S. Chandrasekhar, *Hydrodynamic and hydromagnetic stability* (Oxford, 1961), pp. 9–75
5. J.R.A. Pearson, J. Fluid Mech. **4**, 489 (1958)
6. L.E. Scriven, C.V. Sterling, J. Fluid Mech. **19**, 321 (1964)
7. V. Regnier, P. Dauby, G. Lebon, Phys. Fluids **12**, 2787 (2000)
8. V. Regnier, P. Dauby, G. Lebon, Acta. Astronautica **48**, 617 (2001)
9. S.H. Davis, G.M. Homsy, J. Fluid Mech. **98**, 527 (1980)
10. V. Regnier, G. Lebon, J. Mech. Appl. Math. **48**, 57 (1995)
11. P. Gillon, P. Courville, A. Steinchen-Sanfeld, G. Bertand, M. Lallemant, PCH Physic-Chemical Hydrodynamics **10**, 149 (1987)
12. H.J. Palmer, J. Fluid Mech. **75**, 487 (1975)
13. A. Prosperetti, M.S Plesset, Phys. Fluids **27**, 1590 (1984)
14. J.P. Burelbach, S.G. Bankoff, S.H. Davis, J. Fluid Mech. **195**, 463 (1988)
15. V.M. Ha, C.L. Lai, J. Chinese Inst. Ing. **21**, 547 (1998)